Journal of Inorganic and Organometallic Polymers and Materials (2020) 30:1915–1923
https://doi.org/10.1007/s10904-019-01343-5

Study of Transition Metal Ion Doped CdS Nanoparticles for Removal of Dye from Textile Wastewater

A. Rafiq[1] · M. Imran[2,3] · M. Aqeel[1] · M. Naz[4] · M. Ikram[1] · S. Ali[1,5]

Received: 17 August 2019 / Accepted: 29 September 2019 / Published online: 3 October 2019

Abstract
Simple and cost-effective co-precipitation route was employed to prepare pure and transition metal ions doped CdS nanoparticles using 2-mercaptoethanol as surfactant. Doping of Ni, Co and Fe ions to CdS nanoparticles have been characterized adopting various techniques. X-ray diffraction confirmed CdS has single cubic phase with crystal size varying from 1 to 2 nm. UV–Vis spectroscopy analysis reveals an increase in absorption intensity upon doping. From Raman spectra, small shift in wave number is observed with inclusion of dopants which may be attributed to optical phonon confinement. Scanning electron microscopy confirmed agglomerated spherical morphology and Cd–S linkage along with other related functional groups was recorded by Fourier transform infrared spectroscopy. Photocatalytic measurements of undoped and doped CdS were studied by irradiating methylene blue solution under visible light. It was observed that Co doped CdS effectively bleaches out methylene blue than Ni and Fe doped CdS upon exposure of visible light. This report also highlights effect of prepared nanoparticles in degradation of methylene blue by catalytic agent $NaBH_4$.

Keywords CdS nanoparticles · Doping · Methylene blue · Photocatalytic activity · Catalysis

1 Introduction

Around 100,000 kinds of dyes are produced annually with production rate of over 7×10^5 to 1×10^6 tons and utilized in numerous industries paper, textile, rubber, pigments, plastic, leather and paint [1]. Approximately 10–15% of used dyes discharged into water bodies and surrounding environment causing injurious diseases cancer, skin irritation, disfunction of liver, reproductive system and kidneys in humans [2]. One of the most widely used cationic dye is methylene blue (MB) which is injurious to human beings. This dye causes severe diseases like respiratory tract irritation, eye and skin irritation, permanent injury to conjunctiva and cornea in human beings and rabbit eyes [3]. Discharging of contaminated wastewater by MB per annum causes numerous environmental problems such as increasing demand of chemical oxygen above the expected limit may cause death of the marine life [4, 5].

Various techniques chemical precipitation, conventional coagulation, electrolysis, reverses osmosis from comprising, adsorption and photocatalytic degradation have been explored to purify industrial wastewater by removing dyes [6]. For the removal of dyes, photocatalytic degradation and adsorption are endorsed as environmentally efficient and cheap techniques for dyes removal [7]. Though, adsorption by low-cost materials is effective in dyes removal, however such procedures produce solid wastes substantially [8].

Semiconductor photocatalysis as a green technology for organic contaminants/wastewater treatment and green energy production has attracted substantial attention since Fujishima and Honda realized water splitting to produce hydrogen by TiO_2 in 1972 [9, 10]. Hereafter, several

✉ M. Ikram
dr.muhammadikram@gcu.edu.pk

1 Solar Cell Applications Research Lab, Department of Physics, Government College University Lahore, Punjab 54000, Pakistan

2 Technical Institute of Physics and Chemistry, Chinese Academy of Sciences, 29 Zhongguancun East Road, Haidian District, Beijing 100190, China

3 University of Chinese Academy of Sciences, Beijing 100049, China

4 Biochemistry Lab, Department of Chemistry, Government College University Lahore, Punjab 54000, Pakistan

5 Department of Physics, Riphah Institute of Computing and Applied Sciences (RICAS), Riphah International University, 14 Ali Road, Lahore, Pakistan

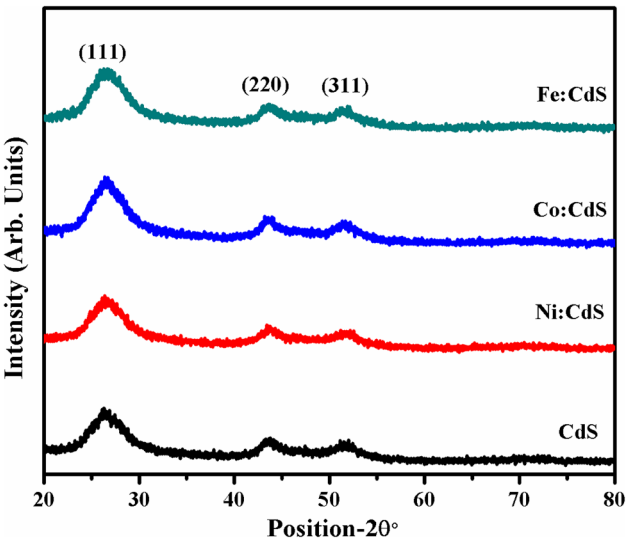

Fig. 1 Crystal structure of pure and doped CdS NPs

photocatalysts, composite structures [11, 12], transition metal oxides [13–15], metal sulfides [16, 17], doping materials [18, 19], heterojunctions [20, 21] have been synthesized to improve photocatalytic activities. But to synthesize high activity and low-cost photocatalysts owing to safety issues and non-secondary pollution to environment is still a challenge. Among hundreds of semiconductor materials known for photocatalytic activity, transition-metal elements are particularly promising materials due to significant optical and electronic properties. Among II–VI compound semiconductors, CdS has been investigated extensively and regarded as a unique photocatalyst [17, 22, 23]. Interestingly, CdS served as a promising candidate for detecting visible radiations [24] and conduction band is more negative relative to reduction potential of H^+/H_2 [25].

The efficacy of CdS for photodegradation is dependent on the integration with appropriate dopant elements. The dopant transition metals to CdS displayed outstanding optical, magnetic and electrical properties as single material [26, 27]. In this study, synthesis of undoped and Fe, Co and Ni doped CdS using chemical precipitation method. These prepared NPs were characterized deploying various analytical tools and utilized as photocatalyst on degradation of MB under visible light irradiation and catalysis in the presence of catalytic agent.

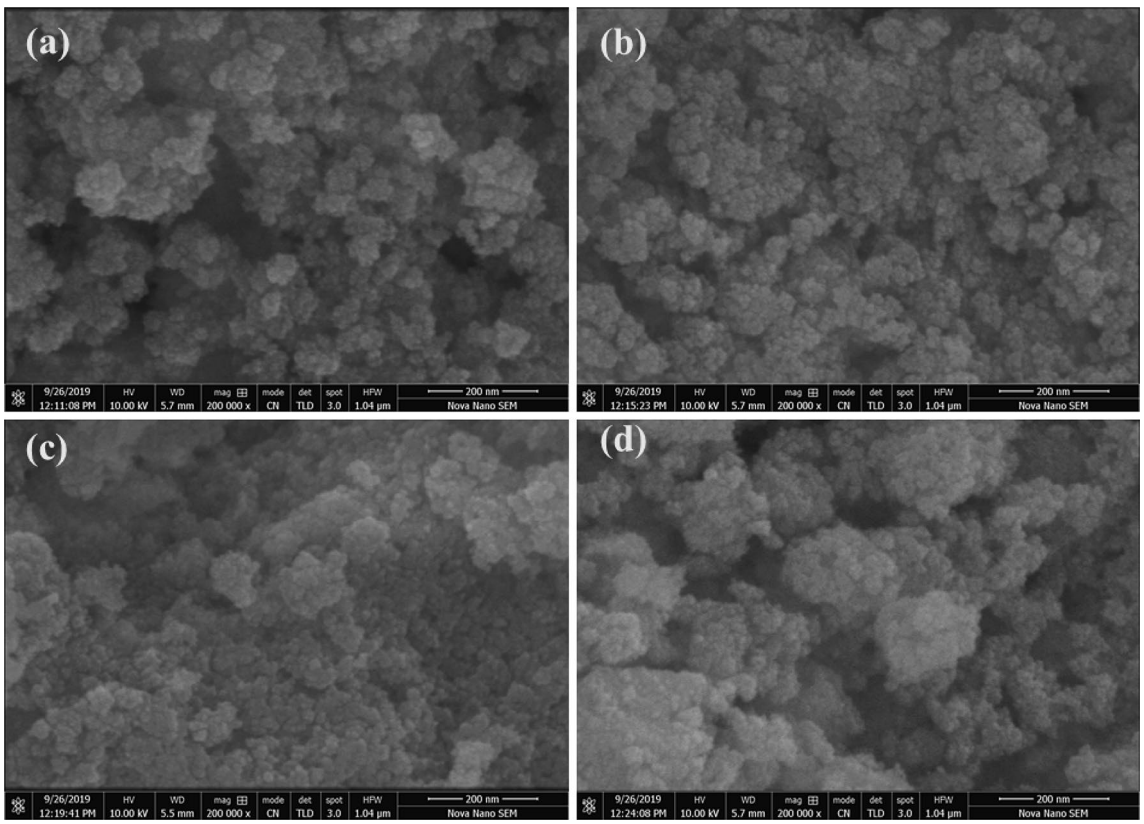

Fig. 2 SEM images of pristine CdS (**a**) and doped (Ni, Co, Fe) CdS (**b**–**d**)

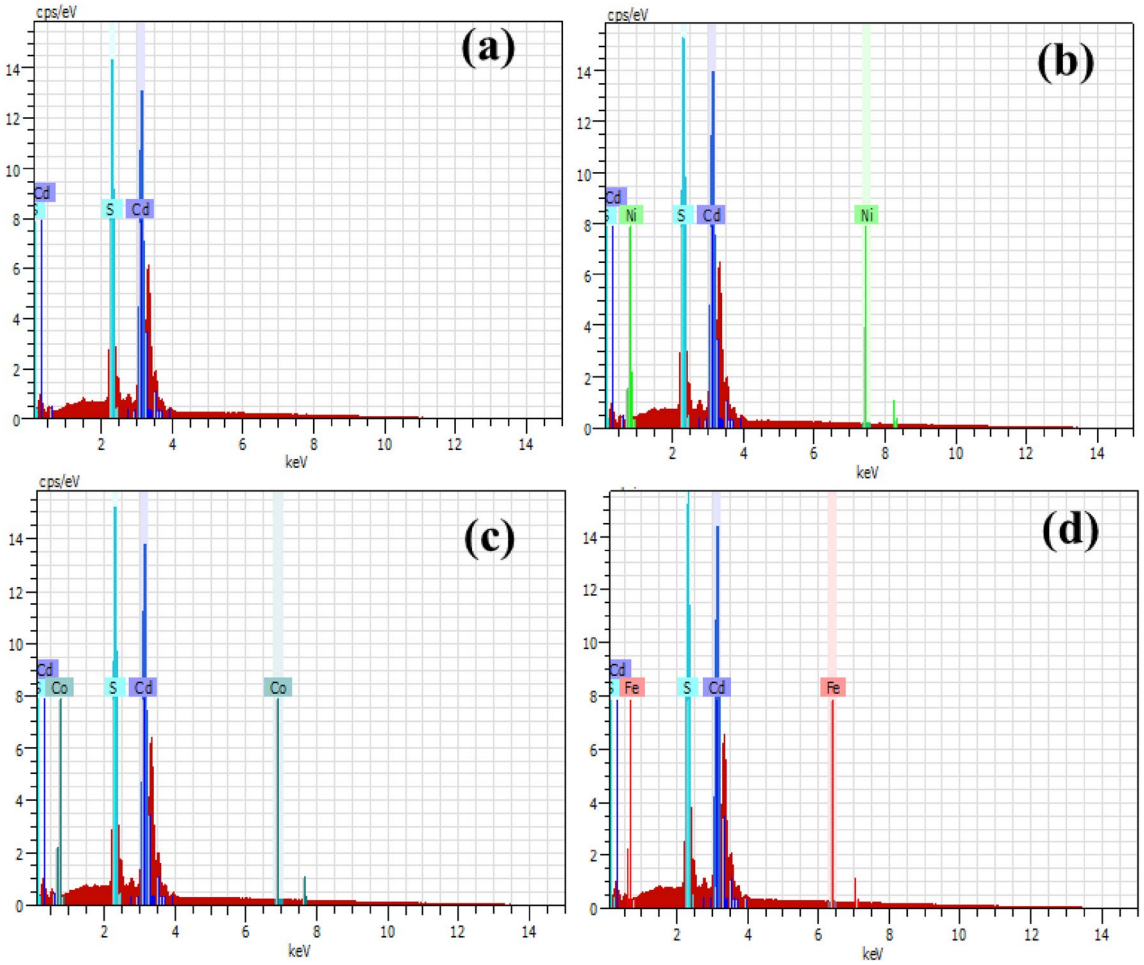

Fig. 3 EDX spectra of pristine CdS (**a**) and doped (Ni, Co, Fe) CdS (**b**–**d**)

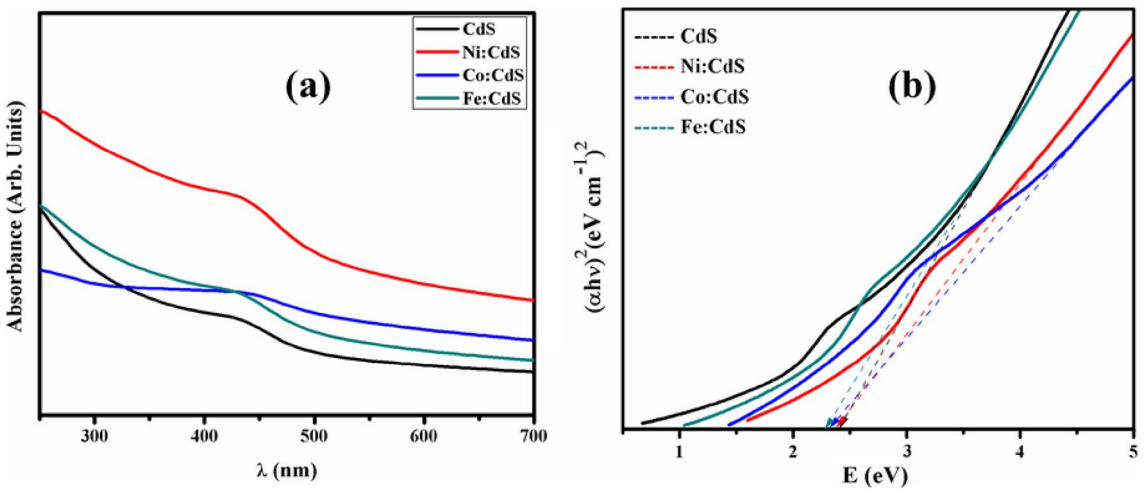

Fig. 4 Absorption spectra (**a**) and corresponding bandgap spectra for pristine and doped (Ni, Co, Fe) CdS (**b**)

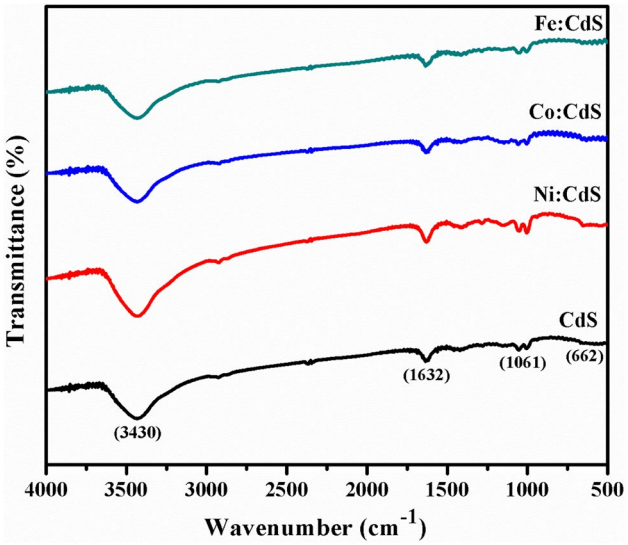

Fig. 5 FTIR spectra of pure and doped CdS NPs

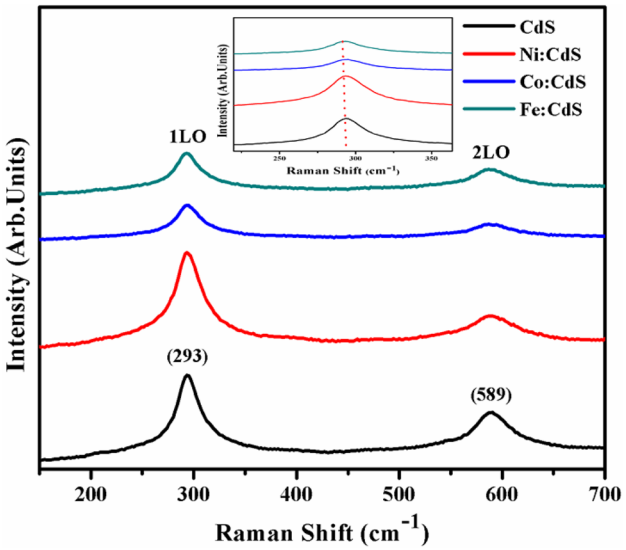

Fig. 6 Raman spectra of pure and doped CdS NPs

2 Experimental Details

2.1 Materials

Cadmium chloride 2,5 hydrate ($CdCl_2{\cdot}2{,}5H_2O$) as Cd source, sodium sulfide pentahydrate ($Na_2S{\cdot}5H_2O$—98%) as a sulfur source, nickel(II) nitrate hexahydrate ($Ni(NO_3)_2{\cdot}6H_2O$—96%), cobalt(II) nitrate hexahydrate ($Co(NO_3)_2{\cdot}6H_2O$—96%) and iron(III) nitrate 9-hydrate ($Fe(NO_3)_3{\cdot}9H_2O$) as a dopant materials salts. Capping agent 2-mercaptoethanol ($HOCH_2CH_2SH$) was acquired from AppliChem. Methylene blue (MB) and sodium borohydride ($NaBH_4$—98.0%) were purchased from BDH Laboratories supplies and Sigma Aldrich, respectively.

2.2 Synthesis of CdS Nanoparticles

Chemical precipitation technique was adopted to prepare pure and doped CdS NPs using 2-mercaptoethanol as a capping agent. 0.1 M solutions of $CdCl_2$ and Na_2S were prepared separately under vigorous stirring in 50 ml deionized water (DIW) for 30 min. Later, Na_2S solution was mixed dropwise in $CdCl_2$ solution. Afterwards, 2.5 ml of 2-mercaptoethanol ($HOCH_2CH_2SH$) solution was mixed slowly to above solution under vigorous stirring at 65 °C. Yellowish precipitates of CdS appeared during drop wise mixing of Na_2S, these precipitates were washed with DIW, filtered and dried at 80 °C for 24 h to obtain nascent CdS. For doping, Ni^{2+}, Co^{2+} and Fe^{2+} (5%) were mixed in $CdCl_2$ solution using above-mentioned procedure.

2.3 Photocatalytic Process

The photocatalytic measurements of prepared samples were tested by UV–Vis spectrophotometer (Genesys 10S spectrophotometer) under visible light irradiation at room temperature. The visible light was generated by a 400 W mercury lamp with principal wavelength of 400–700 nm. 10 mg suspension of synthesized nanocatalysts was dispersed into 70 ml aqueous solution of dye. This suspended solution was stirred magnetically for 30 min in dark to attain adsorption–desorption equilibrium between MB and CdS. After a specified irradiation time interval of visible light exposure, 5 ml suspension was collected for the purpose of UV–Vis spectroscopy analysis. Concentration of MB was evaluated by monitoring changes in dye concentration with irradiation time in UV–Vis spectra.

2.4 Catalytic Process

Sufficient amount of DIW was used to dilute 1 mM solution of MB in quartz cell and mixed 400 µl of $NaBH_4$ solution. Subsequently, 300 µl of as-prepared NPs were added under agitation for 5 min. The dye decolorization signifies reduction in colour upon reducing agent ($NaBH_4$). The absorption spectrum was obtained at regular intervals with principal wavelength of 200–800 nm using UV–Vis spectrophotometer.

2.5 Characterization

X-ray powder diffraction (XRD) PAN Analytical Xpert PRO X-ray diffraction was carried out to examine the different ions doped CdS samples with CuKα radiations at 40 kV.

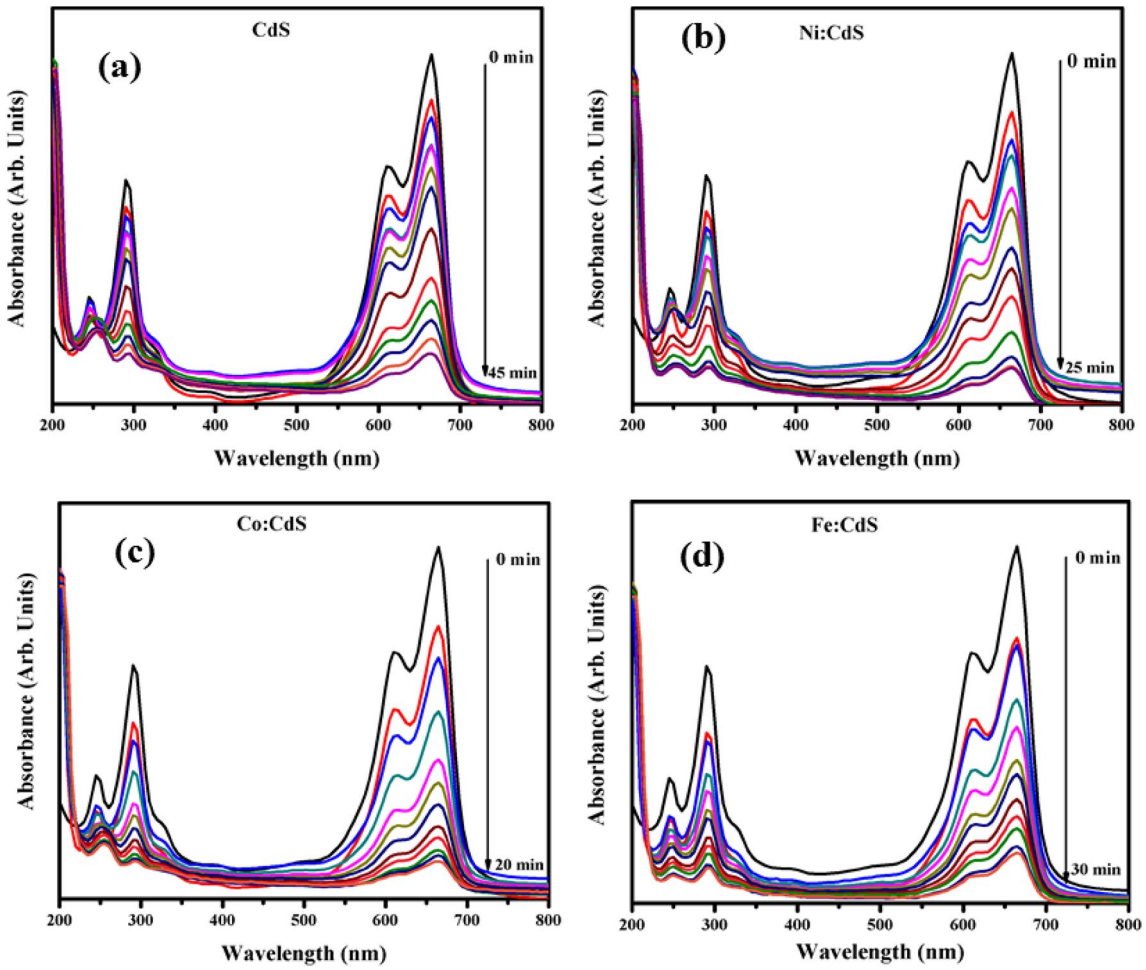

Fig. 7 Time-dependent UV–Vis spectra for reduction of MB. Dye with $NaBH_4$ + CdS (**a**), dye with $NaBH_4$ + Ni:CdS (**b**), Dye with $NaBH_4$ + Co:ZnS (**c**), Dye with $NaBH_4$ + Fe:ZnS

The surface morphologies were investigated by Nova Nano SEM 450 with accelerating voltage of 20 kV. For optical analysis, UV–Vis spectrophotometer (Genesys 10S spectrophotometer) was used. Chemical structure was collected on Fourier Transform Infrared spectroscopy-FTIR (Perkin Elmer spectrometer). Raman spectra were measured with an excitation wavelength of 532 nm using DXR Raman microscope (Thermo Scientific).

3 Results and Discussion

To check the crystallinity, phase and crystal structure of prepared nanopowders, XRD was employed (Fig. 1). Three prominent peaks were observed at 26.5°, 43.5° and 51.6° corresponding to (111), (220) and (311) reflection planes of CdS respectively without impurity [25]. It is observed that diffraction peaks have identical positions and definite broadening of peaks indicates nanometer range of as-prepared materials [24, 25, 28]. As radii of dopants ions are smaller than Cd (108 pm) ion, inclusion of dopants in CdS lattice will decrease lattice constants. Hence, diffraction peaks of doped NPs were observed shifted slightly towards higher angle. The average crystallite size of pristine and doped CdS was measured using Debye–Scherrer formula. The calculated crystallite size values 1.9, 2.01, 2.07 and 2.04 nm with standard deviation < 5% correspond to pure, Ni, Co and Fe dopants, respectively.

Figure 2a–d show SEM micrographs of synthesized pure and doped (Ni, Co, Fe) NPs. Figure 3a shows formation of highly agglomerated CdS nanoparticles. Upon doping, irregular growth of particles appeared due to Ostwald ripening [29, 30].

Figure 3 depicts EDAX analysis from corresponding to elements Cd, S, Ni, Co and Fe confirms the presence of NPs in polymer matrix which specify homogenous doping of impurity ions in CdS structure.

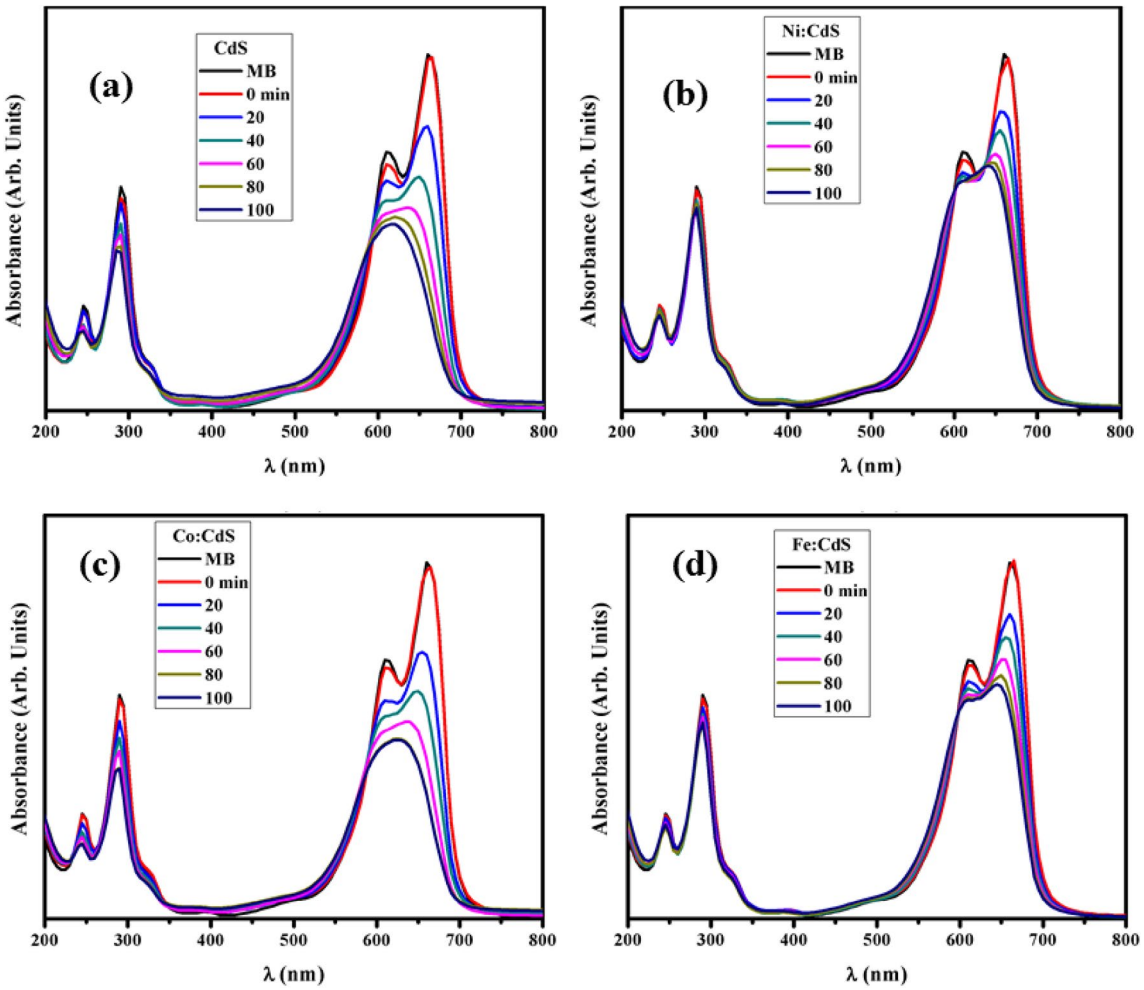

Fig. 8 Time-dependent UV–Vis absorption spectra for decolorization of methylene blue in the presence of pure and doped CdS (**a**–**d**)

Table 1 Comparison of current and reported studies of TM doped CdS NPs

Reported	TM doped ZnS	Synthesis techniques	Particle size (nm)	Band gap (eV)	Photocatalysis
Junaid et al. (2019) [25]	Fe (0–5%) doped CdS	Co-precipitation	11.6–4.4	2.4–2.1	Significant increase in photocatalytic activity upon 5% Fe doping
Chauhan et al. (2013) [24]	Fe (0, 3, 5 and 10%) doped CdS	Chemical route	2–3	2.3–2.2	3% Fe doped CdS NPs exhibit higher degradation efficiency.
Patel et al. (2015) [40]	Ni (0, 10, 15 and 20%) doped CdS	Chemical synthesis	3–6	X	X
Present study	Ni, Co and Fe (5%) doped CdS	Co-precipitation	1–2	2.4–2.3	Photocatalytic measurements reveal higher degradation rate for Co doped ZnS

Optical properties of nanopowders were explored using UV–Vis spectroscopy as shown in Fig. 4. Intensive absorption peak of pristine CdS was observed near 440 nm [25]. However, absorption intensity increased upon doping. This increase in absorption may be attributed to increase in carrier concentration by dopant ions incorporation and creation of defect levels in band gap. Compared to bulk CdS, blue shift in absorption edge appears, indicating that prepared NPs lie in nanometer range [31]. Energy band gap of NPs was measured using Tauc's equation and found to be 2.4 eV of

CdS which is well matched with reported [25] (Fig. 4b). A decrease in bandgap was observed with incorporation of Ni, Co and Fe dopants from 2.38 to 2.30 eV [24].

FTIR spectra of pristine and doped CdS were recorded in the range 4000 to 500 cm^{-1} as depicted in Fig. 5. Broad peak at 3434 cm^{-1} is associated to O–H group, confirms affinity of water molecules towards CdS [32, 33]. Peaks around 1544 cm^{-1} and 1627 cm^{-1} attributed to C–O and C=C stretching modes of carbonyl and carboxyl groups [28, 34, 35]. During synthesis of NPs, adsorption of CO_2 and H_2O can contribute from atmosphere [33]. Moreover, shoulder at 662 cm^{-1} depicts presence of Cd–S bond stretching seems very weak because of sample moisture [36]. Absorption peak around 2800–2900 cm^{-1} corresponds to C–H stretching [37]. Interestingly, no change in peak positions of matrix was observed with inclusion of dopants in CdS network. This confirms that dopants crystallites are formed without disturbing the continuous three-dimensional network of CdS and independent in chemical behavior [38].

Figure 6 depicts Raman spectra of NPs recorded at room temperature. Raman peaks appeared at 293 and 589 cm^{-1} associated to 1LO (longitudinal optical) and 2LO phonon modes which show consistency with earlier reported values [25, 39, 40]. The Raman spectra of doped CdS NPs display a slight shift in wave number of 1LO and 2LO when compared with pristine CdS, which is accredited to smaller difference in ionic radii of dopants than Cd^{2+} [41].

Figure 7 shows catalytic reduction of MB using $NaBH_4$ with CdS NPs as nano-catalysts. The extracted results indicate that CdS shows successive decrease in concentration of dye within 45 min while doped nano-catalysts reveal enhanced degradation. Degradation efficiency of Ni and Co doped CdS is higher than Fe as these nano-catalysts reduced dye within 25 and 20 min, respectively at peak intensity of ≈664 nm. Pure CdS shows slower reduction of dye, indicating superior catalytic function of doped CdS. Hence, doped NPs were proved as promising catalysts on degradation of MB from industrial effluents.

Photocatalytic activity of CdS catalysts was subsequently evaluated under visible light irradiation by monitoring MB discoloration in aqueous solution. With increasing illumination time, peak maxima of MB absorbance spectra at 664 nm decreases gradually (Fig. 8) [42]. Successive MB degradation with prepared catalysts can be associated to crystal defects that behave as recombination centers to decrease photocatalytic performance [25]. Results reveal that MB photo degradation rate in Co doped CdS sample was higher in comparison of other CdS catalysts. This agrees well with an earlier study on metals doped CdS catalysts where faster degradation rate of MB with using Co doped CdS NPs was attributed to increase in defect sides generated by Co doping, and optical absorption is increased in visible region [43]. Reduction of dye was investigated spectrophotometrically by monitoring absorption maximum at 664 nm with definite time intervals. Additionally, CdS displayed inverse degradation in comparison of doped samples [24]. Table 1 shows comparison between recent and reported studies regarding various TM ions doped CdS NPs.

4 Conclusion

In this study, pure and Ni, Co, Fe doped CdS NPs ($Cd_{1-x}TM_xS$ where x = 0.05) were successfully prepared using co-precipitation method. XRD revealed that pure and doped NPs exhibit cubic phase with measure crystallite sizes ranging from 1.9 to 2.07 nm. SEM images showed higher agglomeration in doped nanoparticles than ZnS and FTIR confirmed stretching vibrations of Cd–S around 662 cm^{-1} and other associated functional groups. The optical measurement of undoped and doped ZnS shows that absorption increased and corresponding measured band gap decreased upon doping from 2.38 to 2.30 eV. Doped NPs are significant catalyst due to fast reduction of MB in the presence of reducing agent as compared to CdS. Additionally, Co doped NPs showed higher photocatalytic activity than rest of samples. This novel approach of doped CdS NPs offers an efficient approach to tackle removal of dyes from wastewater and provide an economic route to environmental protection.

Acknowledgements Authors are thankful to higher education commission HEC-Pakistan through start research Grant Project No. 21-1669/SRGP/R&D/HEC/2017.

Compliance with Ethical Standards

Conflict of interest Authors confirm that this manuscript has no conflict of interest.

References

1. S. Chowdhury, P. Saha, Adsorption kinetic modeling of safranin onto rice husk biomatrix using pseudo-first-and pseudo-second-order kinetic models: comparison of linear and non-linear methods. CLEAN–Soil Air Water **39**(3), 274–282 (2011)
2. Yahya S. Al-Degs, Musa I. El-Barghouthi, Amjad H. El-Sheikh, Gavin M. Walker, Effect of solution pH, ionic strength, and temperature on adsorption behavior of reactive dyes on activated carbon. Dyes Pigments **77**(1), 16–23 (2008)
3. Vinod K. Gupta, Dinesh Mohan, Vipin K. Saini, Studies on the interaction of some azo dyes (naphthol red-J and direct orange) with nontronite mineral. J. Colloid Interface Sci. **298**(1), 79–86 (2006)
4. M. Shaban, A.M. Ashraf, M.R. Abukhadra, TiO_2 nanoribbons/carbon nanotubes composite with enhanced photocatalytic activity; fabrication, characterization, and application. Sci. Rep. **8**(1), 781 (2018)

5. A. Al-Kdasi, A. Idris, K. Saed, C.T. Guan, Treatment of textile wastewater by advanced oxidation processes—a review. Global Nest: Int. J **6**(3), 222–230 (2004)
6. A. Wang, Y. Wang, W. Yu, Z. Huang, Y. Fang, L. Long, Y. Song et al., TiO_2–multi-walled carbon nanotube nanocomposites: hydrothermal synthesis and temporally-dependent optical properties. RSC Adv **6**(24), 20120–20127 (2016)
7. M. Sivakumar, A. Towata, K. Yasui, T. Tuziuti, T. Kozuka, Y. Iida, Dependence of sonochemical parameters on the platinization of rutile titania—an observation of a pronounced increase in photocatalytic efficiencies. Ultrason. Sonochem. **17**(3), 621–627 (2010)
8. A. Bhatnagar, A.K. Minocha, Conventional and non-conventional adsorbents for removal of pollutants from water—a review. Indian J. Chem. Technol. **13**, 203–217 (2006)
9. A. Fujishima, K. Honda, Electrochemical photolysis of water at a semiconductor electrode. Nature **238**(5358), 37 (1972)
10. C. Chen, W. Ma, J. Zhao, Semiconductor-mediated photodegradation of pollutants under visible-light irradiation. Chem. Soc. Rev. **39**(11), 4206–4219 (2010)
11. K. Fu, J. Huang, N. Yao, X. Xu, M. Wei, Enhanced photocatalytic activity of TiO_2 nanorod arrays decorated with CdSe using an upconversion TiO_2: Yb^{3+}, Er^{3+} thin film. Ind. Eng. Chem. Res. **54**(2), 659–665 (2015)
12. K. Fu, J. Huang, N. Yao, X. Xu, M. Wei, Enhanced photocatalytic activity based on composite structure with downconversion material and graphene. Ind. Eng. Chem. Res. **55**(6), 1559–1565 (2016)
13. X. Xu, T. Zhai, M. Shao, J. Huang, Anodic formation of anatase TiO_2 nanotubes with rod-formed walls for photocatalysis and field emitters. Phys. Chem. Chem. Phys. **14**(47), 16371–16376 (2012)
14. J.C. Park, J. Kim, H. Kwon, H. Song, Gram-scale synthesis of Cu2O nanocubes and subsequent oxidation to CuO hollow nanostructures for lithium-ion battery anode materials. Adv. Mater. **21**(7), 803–807 (2009)
15. P. Basnet, Y. Zhao, Tuning the Cu x O nanorod composition for efficient visible light induced photocatalysis. Catal. Sci. Technol. **6**(7), 2228–2238 (2016)
16. A. Rafiq, M. Imran, M. Ikram, M. Naz, M. Aqeel, H. Majeed, S.G. Hussain, S. Ali, Photocatalytic and catalytic degradation of organic dye by uncapped and capped ZnS quantum dots. Mater. Res. Express **6**(5), 055801 (2019)
17. J. Kundu, D. Pradhan, Controlled synthesis and catalytic activity of copper sulfide nanostructured assemblies with different morphologies. ACS Appl. Mater. Interfaces. **6**(3), 1823–1834 (2014)
18. X. Deng, Q. Zhang, E. Zhou, C. Ji, J. Huang, M. Shao, M. Ding, X. Xu, Morphology transformation of Cu_2O sub-microstructures by Sn doping for enhanced photocatalytic properties. J. Alloys Compd. **649**, 1124–1129 (2015)
19. X. Wan, X. Liang, C. Zhang, X. Li, W. Liang, H. Xu, S. Lan, S. Tie, Morphology controlled syntheses of Cu-doped ZnO, tubular Zn (Cu) O and Ag decorated tubular Zn (Cu) O microcrystals for photocatalysis. Chem. Eng. J. **272**, 58–68 (2015)
20. W. He, C. Wang, F. Zhuge, X. Deng, X. Xu, T. Zhai, Flexible and high energy density asymmetrical supercapacitors based on core/shell conducting polymer nanowires/manganese dioxide nanoflakes. Nano Energy **35**, 242–250 (2017)
21. F. Dong, Z. Zhao, T. Xiong, Z. Ni, W. Zhang, Y. Sun, W.-K. Ho, In situ construction of g-C_3N_4/g-C_3N_4 metal-free heterojunction for enhanced visible-light photocatalysis. ACS Appl. Mater. Interfaces. **5**(21), 11392–11401 (2013)
22. J. He, L. Chen, Z.-Q. Yi, C.T. Au, S.-F. Yin, CdS nanorods coupled with WS_2 nanosheets for enhanced photocatalytic hydrogen evolution activity. Ind. Eng. Chem. Res. **55**(30), 8327–8333 (2016)
23. X. Deng, C. Wang, H. Yang, M. Shao, S. Zhang, X. Wang, M. Ding, J. Huang, X. Xu, One-pot hydrothermal synthesis of CdS decorated CuS microflower-like structures for enhanced photocatalytic properties. Sci. Rep. **7**(1), 3877 (2017)
24. R. Chauhan, A. Kumar, R.P. Chaudhary, Visible-light photocatalytic degradation of methylene blue with Fe doped CdS nanoparticles. Appl. Surf. Sci. **270**, 655–660 (2013)
25. M. Junaid, M. Imran, M. Ikram, M. Naz, M. Aqeel, H. Afzal, H. Majeed, S. Ali, The study of Fe-doped CdS nanoparticle-assisted photocatalytic degradation of organic dye in wastewater. Appl. Nanosci. (2019). https://doi.org/10.1007/s13204-018-0933-3
26. K.S. Rathore, Deepika, D. Patidar, N.S. Saxena, K. Sharma. Cadmium sulphide nanocrystallites: synthesis, optical and electrical studies. In *AIP Conference Proceedings*, vol. 1249, No. 1 (AIP, 2010), pp. 145–148
27. S. Kumar, J.K. Sharma, Effect of nickel doping on optical properties of CdS nanoparticles synthesized via Co-precipitation technique. Mater. Sci. Res. India **14**(1), 5–8 (2017)
28. S. Kumar, S. Kumar, S. Jain, N.K. Verma, Magnetic and structural characterization of transition metal co-doped CdS nanoparticles. Appl. Nanosci. **2**(2), 127–131 (2012)
29. R.A. Devi, M. Latha, S. Velumani, G. Oza, P. Reyes-Figueroa, M. Rohini, I.G. Becerril-Juarez, J.-H. Lee, J. Yi, Synthesis and characterization of cadmium sulfide nanoparticles by chemical precipitation method. J. Nanosci. Nanotechnol. **15**(11), 8434–8439 (2015)
30. K.R. Desai, A.A. Pathan, C.P. Bhasin, Synthesis, characterization of cadmium sulphide nanoparticles and its application as photocatalytic degradation of congored. Int. J. Nanomater. Chem. **3**, 39 (2017)
31. L. Saravanan, A. Pandurangan, R. Jayavel, Synthesis of cobalt-doped cadmium sulphide nanocrystals and their optical and magnetic properties. J. Nanoparticle Res. **13**(4), 1621–1628 (2011)
32. R. Seoudi, S.H.A. Allehyani, D.A. Said, A.R. Lashin, A. Abouelsayed, Preparation, characterization, and size control of chemically synthesized CdS nanoparticles capped with poly (ethylene glycol). J. Electron. Mater. **44**(10), 3367–3374 (2015)
33. N. Qutub, B.M. Pirzada, K. Umar, S. Sabir, Synthesis of CdS nanoparticles using different sulfide ion precursors: formation mechanism and photocatalytic degradation of Acid Blue-29. J. Environ. Chem. Eng. **4**(1), 808–817 (2016)
34. A.A. Ziabari, F.E. Ghodsi, Growth, characterization and studying of sol–gel derived CdS nanoscrystalline thin films incorporated in polyethyleneglycol: effects of post-heat treatment. Sol. Energy Mater. Sol. Cells **105**, 249–262 (2012)
35. A.E. Vikraman, A.R. Jose, M. Jacob, K.G. Kumar, Thioglycolic acid capped CdS quantum dots as a fluorescent probe for the nanomolar determination of dopamine. Anal. Methods **7**(16), 6791–6798 (2015)
36. N. Qutub, S. Sabir, Optical, thermal and structural properties of CdS quantum dots synthesized by a simple chemical route. Int. J. Nanosci. Nanotechnol. **8**(2), 111–120 (2012)
37. K.P. Tiwari, F. AIi, R.K. Mishra, S. Kumar, K. Sharma, Study of structural, morphological and optical properties of Cu and Ni dopes CdS nanoparticles prepared by microwave assisted solvo thermal method. Digest J. Nanomater. Biostruct. (DJNB) **14**(2) (2019)
38. N. Kumar, L.P. Purohit, Y.C. Goswami, Spin coating of highly luminescent Cu doped CdS nanorods and their optical structural characterizations. Chalcogenide Lett. **12**(6), 333–338 (2015)
39. M. Thambidurai, N. Muthukumarasamy, S. Agilan, N. Murugan, N. Sabari Arul, S. Vasantha, R. Balasundaraprabhu, Studies on

optical absorption and structural properties of Fe doped CdS quantum dots. Solid State Sci. **12**(9), 1554–1559 (2010)
40. N.H. Patel, M.P. Deshpande, S.H. Chaki, Study on structural, magnetic properties of undoped and Ni doped CdS nanoparticles. Mater. Sci. Semicond. Process. **31**, 272–280 (2015)
41. M. Thambidurai, N. Muthukumarasamy, S. Agilan, N. Sabari Arul, N. Murugan, R. Balasundaraprabhu, Structural and optical characterization of Ni-doped CdS quantum dots. J. Mater. Sci. **46**(9), 3200–3206 (2011)
42. Z. Lei, Z.-D. Meng, K.-Y. Cho, W.-C. Oh, Synthesis of CdS/CNT-TiO_2 with a high photocatalytic activity in photodegradation of methylene blue. New Carbon Mater. **27**(3), 166–174 (2012)
43. I.F. Ertis, I. Boz, Synthesis and characterization of metal-doped (Ni Co, Ce, Sb) CdS catalysts and their use in methylene blue degradation under visible light irradiation. Mod. Res. Catal. **6**, 1–14 (2017)